

Clusters and Colloidal Metals in Catalysis¹

I. I. Moiseev and M. N. Vargaftik

Kurnakov Institute of General and Inorganic Chemistry, Russian Academy of Sciences, Moscow, Russia

Received October 25, 2001

Abstract—The review summarizes the results of works on the synthesis, structure, and magnetic and catalytic properties of giant palladium clusters, specifically, nanosized palladium complexes stabilized by *o*-phenanthroline and acetate ligands, which are objects of the colloid chemistry of palladium.

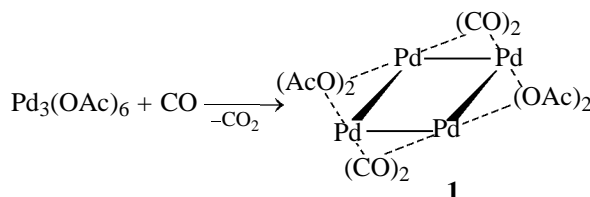
INTRODUCTION

The first metal sol, the sol of gold, obtained by Faraday [1] by reduction of AuCl_4 with white phosphorus in aqueous solution, appeared a bit earlier than the term “colloid” introduced by Graham in 1861 [2]. Nowadays, this field of chemistry comprises numerous spongy-black metals and, as they supposed very recently [3], “suspensions” of metals, such as gold, silver, palladium, platinum, etc. Later the “suspension” of gold, prepared by Faraday, was shown to consist of nanoparticles (with the metal core size of 3 to 30 nm). Closely related to this class of compounds are large metal clusters including more than 100 metal atoms in their framework. There is no principal difference between large clusters and colloidal metals. However, the smaller the cluster size, the more details of the cluster structure are recognizable. For this reason, it would be correct not to divide the objects of that section of colloid chemistry into clusters and colloids, but to speak about thoroughly and poorly studied colloidal systems.

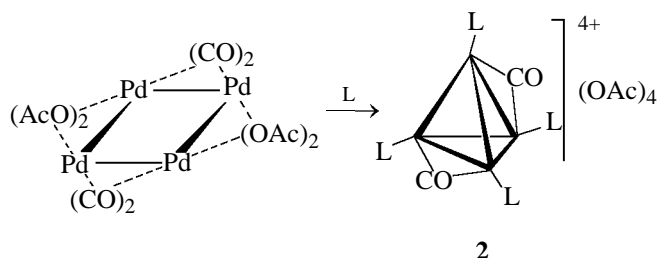
This article presents the results of research into the so-called “giant clusters”² of palladium, whose nucleus comprises about 600 metal atoms.

SYNTHESIS OF GIANT PALLADIUM CLUSTERS

The first samples of catalytically active giant clusters were synthesized starting from the tetranuclear palladium cluster $\text{Pd}_4(\text{CO})_4(\text{OAc})_4$ (**1**) that is formed by reaction of Pd^{II} acetate with CO [6].



In this cluster, the ligands CO and OAc are easily substituted by other soft bases L, such as triphenyl phosphine (PPh_3), 1,10-phenanthroline (phen), or 4,4'-dipyridyl (dipy). With excess ligand L, stable, catalytically inert cationic clusters like **2** were obtained, whose structure was determined by X-ray diffraction analysis [7].



With insufficient ligand L, high-molecular colloid-like Pd-containing products of condensation of primary clusters like **2** are formed, possessing a high catalytic activity in oxidation and hydrogenation of unsaturated compounds [8].

Substances close in composition and catalytic properties were obtained starting from a trinuclear Pd^{II} acetate by successive treatment of a solution of $\text{Pd}_3(\text{OAc})_6$ in acetic acid, containing small amounts ($\leq 1/2$ mol/at. Pd) of phen or dipy, with gaseous H_2 and O_2 [4, 5]. The resulting substances turned to be unique, in terms of activity and selectivity, catalysts for redox and acid–base reactions of organic compounds: olefins, alkylarenes, nitroarenes, nitriles, CO, and alcohols [8].

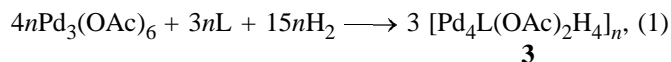
¹ Devoted to Academician Anatoly Ivanovich Rusanov in acknowledgement of his outstanding contribution to physical and colloid chemistry.

² The term was proposed by the authors of the present work in [4, 5].

By contrast to cluster **2**, the latter catalytically active clusters were obtained in the form of X-ray amorphous powders, and their single crystals suitable for X-ray diffraction analysis could not be grown. Therefore, the chemical nature and structure of these substances were assessed in a way unusual for coordination chemistry, by a comparison of data of various indirect methods. Some of these methods, such as NMR, magnetochemistry, elemental analysis, small-angle X-ray scattering (SAXS), thermogravimetry, and ultracentrifugation in solutions, were earlier used in coordination or colloid chemistry. Other newer methods and their modifications have become accessible in recent years: EXAFS, broad-band magic angle spinning NMR (MAS NMR), high (atomic)-resolution electron microscopy (HREM), electron diffraction of single nanoparticles, scanning tunnel microscopy (STM), etc. On every stage of investigation, the chemical composition of clusters was thoroughly controlled by elemental analysis for C, H, N, and Pd.

STRUCTURE OF GIANT PALLADIUM CLUSTERS

Reduction of Pd^{II} acetate (1 at H₂, 20°C, solution in acetic acid, L: Pd = 1:2) gives rise to a precursor of the giant cluster, whose composition, by elemental analysis and ¹H NMR spectroscopy, corresponds to the simplest formula Pd₄phen(OAc)₂ (**3**):

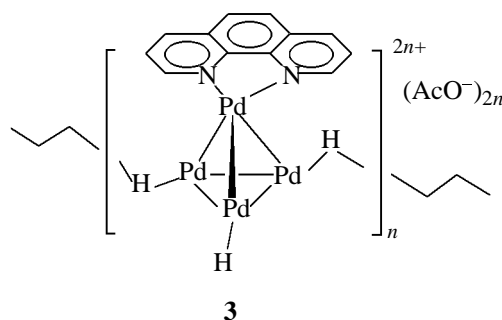


$$n \approx 100, \text{ L} = \text{phen or dipy}.$$

According to transmission electron microscopy (HREM), electron diffraction, and SAXS data [9], the metal core of complex **3** has an almost spherical shape with a diameter of 20 ± 4 Å. Analysis of the extended X-ray absorption fine structure (EXAFS) Pd *K*-edge of complex **3** revealed only two maxima in the curve of radial distribution of atoms. One of the maxima (2.1 ± 0.1 Å) corresponds to the distance between Pd and a light atom (N or O), and the second (2.6 ± 0.1 Å), to the Pd–Pd distance.

The available evidence (elemental analysis, NMR, electron microscopy, and EXAFS) and certain analogies with clusters **2** led us to conclude [12, 13] that the polymeric molecules of complex **3** consist of coiled chains formed by the elementary tetrahedral clusters ...{[(Pd₄H₃L)H]²⁺(OAc[−])₂}....

Under the action of O₂, complex **3** eliminates hydride atoms and transforms to a stable polynuclear complex with the simplest formula Pd₉phen(OAc)₃



(**4**) readily soluble in water and aqueous-organic media [4, 5]. The molecular weight of complex **4**, measured by the method of ultracentrifugation in solution, turned to be (1.0 ± 0.5) × 10⁵.

A more exact assessment the shape and size of cluster molecules **4** was obtained by means of transmission electron microscopy (TEM) and SAXS (Fig. 1), as well as electron diffraction. The metal core of cluster **4** is observed in electronic microphotographs as almost spherical particles with a diameter of 26 ± 3.5 Å. According to SAXS data, the average diameter of molecules **4** is 20 ± 5 Å, whereas the estimate from the half-widths of diffraction rings is ~25 Å [10, 11].

The information on the structure of the metal core of cluster **4** was obtained by means of EXAFS and transmission electron microscopy (TEM, HREM). The curve of radial distribution of atoms, calculated from the EXAFS spectrum, contains four Pd–Pd interatomic distances within the range 2.6 to 4 Å, which coincides with the expected set of P–Pd distances for an icosahedral packing of metal atoms (Table 1).

The HREM study showed the presence of particles with three different types of packing of Pd atoms in the samples of cluster **4**: (1) face-centred cubic; (2) icosahedral, and (3) dense packing with no long-range order in the location of metal atoms in the core [12–14].

On the ground of data on the size of the metal core of the cluster, the character of packing of Pd atoms, and Pd–Pd distances, a conclusion was drawn that the metal core of cluster **4** contains 570 ± 30 palladium atoms. In view of this result and the elemental analysis of the cluster, it was assigned the molecular formula Pd_{570 ± 30}phen_{63 ± 3}(OAc)_{190 ± 10} [4, 5, 10]. This composition (within experimental error) is nicely consistent with the model of a cluster containing a densely packed metal core with one of the “magic” numbers (by Chini’s classification [15]) of Pd atoms.

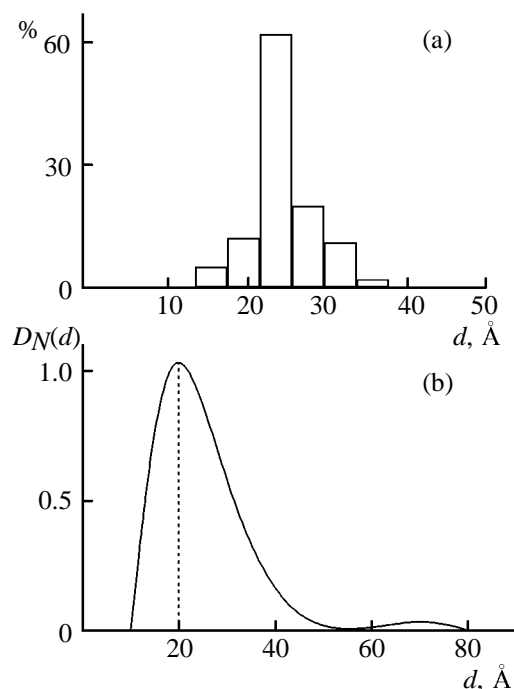


Fig. 1. Distribution of metal cores of cluster **4** as given by electron microscopy (*a*, \bar{d} 26 ± 3.5 Å) and small-angle X-ray scattering (*b*, \bar{d} 20 ± 5 Å).

At such a packing, the number of atoms forming a 12-vertex metal polyhedron is determined by the known equations [16, 17]:

$$N_i = 10i^2 + 2,$$

$$N_\Sigma = 1/3(10m^3 + 15m^2 + 11m + 3),$$

where N_i is the number of metal atoms in the i th densely packed layer around the central atom of the metal polyhedron, i is the layer number, N_Σ is the total

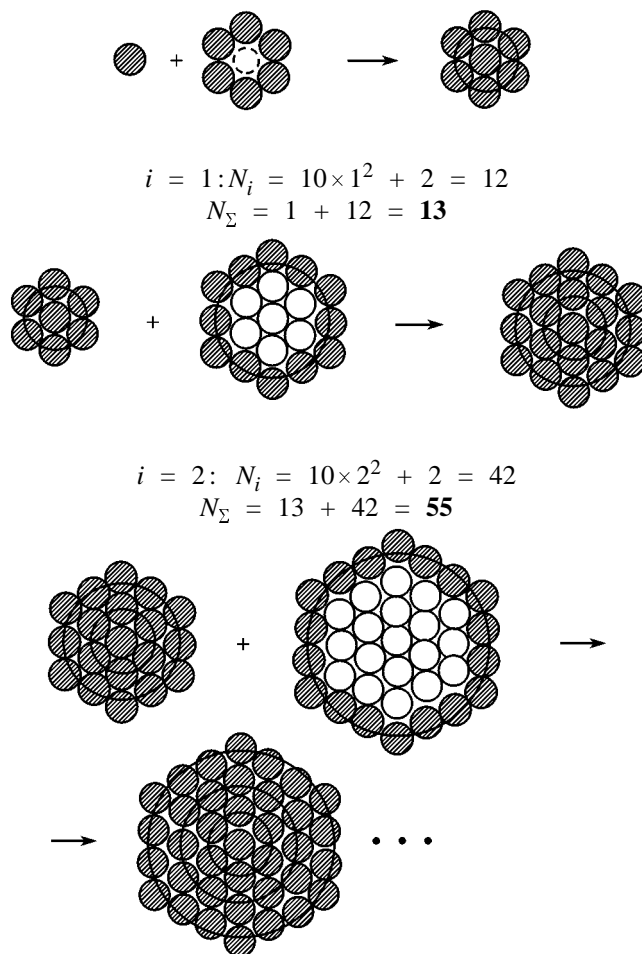
Table 1. Interatomic distances Pd–Pd in the metal core of cluster **4** by EXAFS data, compared with distances expected for other packings of Pd atoms [4]

Packing	Pd–Pd distances, Å				
	2.60±0.04	3.1±0.1	3.66±0.1	4.08±0.1	–
EXAFS data					
	Expected distances ^a				
Face-centered cubic	2.60	–	3.66	–	–
Hexagonal	2.60	–	3.66	–	4.50
Icosahedral	2.60	3.10	3.66	4.10	–

^a Shortest Pd–Pd distance 2.60 Å.

number of atoms in the metal polyhedron, and m is the total number of densely packed layers. Any cluster that meets the above conditions contains a “magic number” of atoms in the metal core (Scheme 1) [15–17].

Scheme 1.
Successive formation of densely packed metal core of 12-vertex giant clusters



$$i = 1: N_i = 10 \times 1^2 + 2 = 12$$

$$N_\Sigma = 1 + 12 = 13$$

$$i = 2: N_i = 10 \times 2^2 + 2 = 42$$

$$N_\Sigma = 13 + 42 = 55$$

$$i = 3: N_i = 10 \times 3^2 + 2 = 92$$

$$N_\Sigma = 55 + 92 = 147 \text{ etc.}$$

$$N_\Sigma = 13 (m = 1), 55 (m = 2), 147 (m = 3), 309 (m = 4), 561 (m = 5), 923 (m = 6), 1415 (m = 7), 2057 (m = 8), 2869 (m = 9) \dots$$

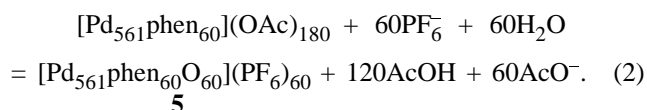
In an idealized model, such a nucleus is constructed as a regular 5-layer 12-vertex polyhedron containing $1 + 12 + 42 + 92 + 162 + 252 = 561$ metal atoms. Thus, the idealized formula of cluster **4** can be represented as $\text{Pd}_{561}\text{phen}_{60}(\text{OAc})_{180}$ (Fig. 2).

The idealized formula corresponds to averaged

values of the size, shape, and composition of cluster **4**. In reality, a giant cluster is not an individual substance of a strictly defined composition, but a set of particles close in composition and structure and more or less approaching the idealized model. In other words, there is a distribution (although narrow enough) of cluster molecules in shape, size, and composition (Fig. 1).

In the idealized model of a Pd-561 cluster, the outer layer of the metal core contains 252 palladium atoms which are able, in principle, to coordinate various ligands. Analysis of the model shows, however, that only sixty phen molecules can be located on the surface of the metal core in the form of bidentately coordinated ligands.³ Therewith, 180 anions OAc^- serve as outer-sphere ligands located at the periphery of the giant cluster cation $[\text{Pd}_{561}(\text{phen})_{60}]^{180+}$. Similar situation was earlier discovered by X-ray diffraction in the tetranuclear cluster $[\text{Pd}_4(\text{CO})_2\text{phen}_4]^{4+} \cdot (\text{OAc}^-)^4$ (**2**, $L = \text{phen}$) [7], where phen molecules are bound with four vertex Pd atoms, and the anions OAc^- play the role of outer-sphere ligands.

The conclusion about the outer-sphere location of OAc^- is consistent with NMR data [9] and also with the fact that these ligands are readily displaced by other anions (Cl^- , ClO_4^- , PF_6^-). For example, treatment of cluster **4** in water with KPF_6 gives a new cluster with the idealized formula $\text{Pd}_{561}\text{phen}_{60}\text{O}_{60}(\text{PF}_6)_{60}$ (**5**) [18]:



The structure of cluster **5** was established by the same methods as that of cluster **4**. In the metal core of this cluster, Pd atoms have a face-centered cubic packing [10, 18].

Clusters **4** and **5** were studied by scanning tunnel microscopy [19], which allowed assessment of the general shape and dimensions of these clusters, including the ligand shell.

MAGNETIC PROPERTIES OF GIANT CLUSTERS

Unlike the relatively well explored small diamagnetic clusters containing 4 to 38 palladium atoms in their metal core, giant clusters **4** and **5** are paramag-

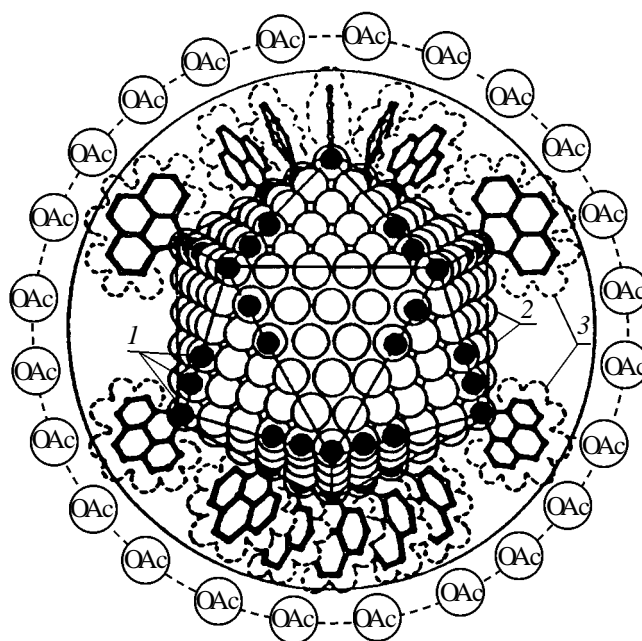


Fig. 2. Idealized structure of the cluster $\text{Pd}_{561}\text{phen}_{60} \cdot (\text{OAc})_{180}$ (**4**): (1) Pd atoms coordinated with phen ligands; (2) Pd atoms accessible for coordination with solvent or substrate molecules; and (3) van der Waals contours of coordinated phen ligands.

netic. Massive palladium possesses the Pauli paramagnetism caused by electrons with energy E_F near the Fermi level, so that the magnetic susceptibility of palladium is almost independent of temperature up to the liquid helium temperature [14, 18]. As found by measurements within the range from room temperature to 77 K, the magnetic susceptibility of giant clusters is 4–5 times lower than for the massive metal, but, similarly to the massive metal, only slightly increases with temperature: $\chi_g(300 \text{ K}) = (+1.3 \pm 0.2) \times 10^{-6}$, $\chi_g(77 \text{ K}) = (+1.8 \pm 0.3) \times 10^{-6}$ CGSU [18]. Thus, as the size of the metal core increases, the Pauli paramagnetism, a typical metallic property, already arises when the cluster nucleus contains at least several hundreds Pd atoms.

An even more interesting behavior of giant clusters we observed in magnetic and heat capacity studies at temperatures close to absolute zero (0.01–1 K) [20]. As the temperature is decreased, the magnetic susceptibility of clusters **4** and **5** first abruptly increases, attaining a maximum at ca. 1 K and then no less abruptly increases to near-zero (Fig. 2). In the same series of experiments we compared the temperature dependence of magnetic susceptibility for larger palladium clusters $\text{Pd}_{1415}\text{phen}_{54}\text{O}_{1000}$ and $\text{Pd}_{2057} \cdot \text{phen}_{78}\text{O}_{1600}$, as well as for the massive metal. It was found that more pronounced deviations from the

³ For steric reasons, these ligands can coordinate to 12 palladium atoms in the vertices of the metal polyhedron and to 2 palladium atoms at each edge adjacent to these vertices.

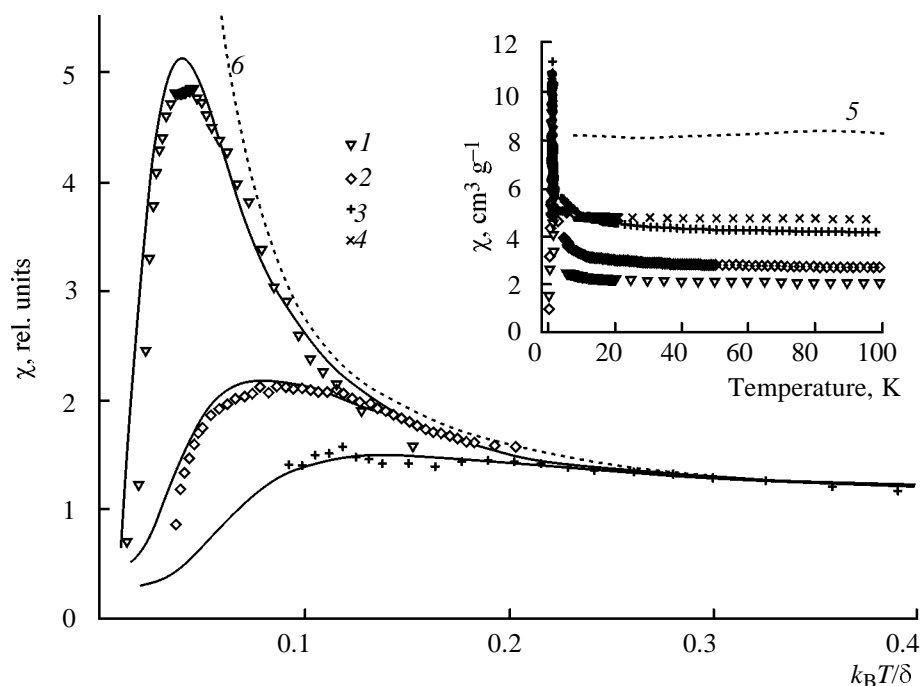


Fig. 3. Electronic magnetic susceptibility of palladium clusters. (1) Cluster with a 5-layer packing of the metal core, $\text{Pd}_{561}\text{Phen}_{60}\text{OAc}_{180}$, (2) 7-layer cluster, (3) 8-layer cluster, (4) poorly characterized palladium black, and (5) compact metal. (6) The dotted line was calculated for the model of quantum-size effect (QSE) at zero field ($B = 0$).

magnetic susceptibility curve for massive palladium are characteristic just of clusters **4** and **5** (Pd_{561}).

Quantum size effects were also revealed in heat capacity studies on giant palladium clusters at extremely low temperatures [20]. As in the case of magnetic susceptibility, the temperature dependence of heat capacity for clusters deviates from the corresponding curve for the massive metal, and the deviation is the larger the less palladium atoms in the metal core of the cluster (Fig. 3).

Thus, giant Pd clusters lie at the boundary beyond which properties of metallic particles become identical with those of the compact metal. Quantum size effects for small particles were earlier predicted theoretically. However, their experimental observation has become possible only after the synthesis of well-described homogeneous clusters with narrow unimodal size and composition distributions, such as giant palladium clusters **4** and **5**.

CATALYTIC PROPERTIES OF GIANT PALLADIUM CLUSTERS

Giant palladium clusters exhibit a high and selective catalytic activity in various chemical reactions (Scheme 2).

Oxidation of alkenes. Giant palladium clusters **4**

and **5** effectively catalyze, under mild conditions (293–363 K, 0.1 MPa) oxidative acetoxylation of alkenes and alkylarenes with a selectivity of 95–98%. By contrast to industrial heterogeneous catalysts acting at considerably higher temperatures, giant clusters do not promote undesirable side transformations of substrates and are insensitive to the water forming in the course of reaction [10, 21].

Kinetic studies on the oxidative acetoxylation of ethylene and propylene (Un) showed [10] that, in solutions containing clusters **4** and **5** (clust), the reaction rate obeys a Michaelis–Menten kinetic equation:

$$r_0 = k[\text{clust}] \frac{[\text{Un}][\text{O}_2][\text{AcOH}]}{(K_I + [\text{Un}]) (K_{II} + [\text{O}_2]) (K_{III} + [\text{AcOH}])}. \quad (3)$$

As follows from the resulting values of Michaelis constants K_I and K_{II} (Table 3), propylene coordinates with giant clusters weaker than ethylene and O_2 .

Further information on the mechanism of olefin oxidation in the presence of giant palladium clusters was gained from experiments on the H/D isotope kinetic effects of substrate and solvent (Table 3) and on inhibited oxidation in the presence of free ligands.

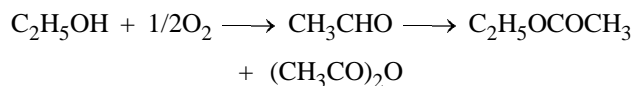
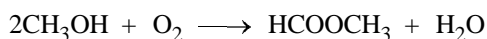
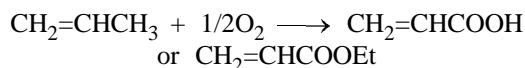
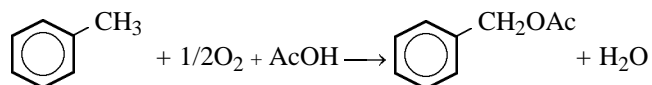
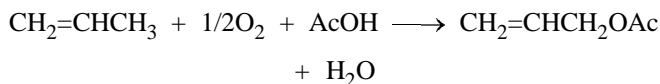
The inhibition data (Fig. 4) show that addition to

Scheme 2.

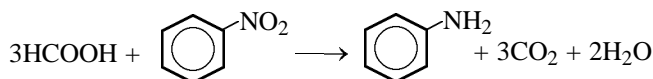
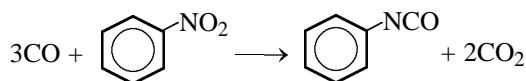
Reactions catalyzed by giant palladium clusters

Oxidation

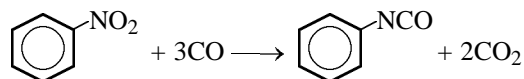
(a) with oxygen



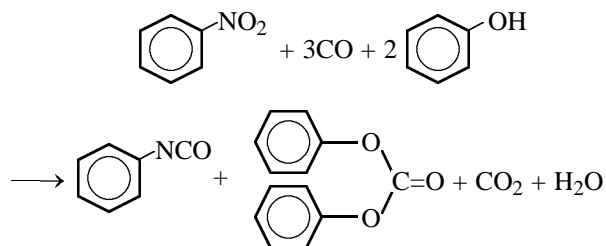
(b) with nitrobenzene



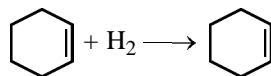
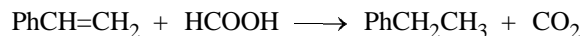
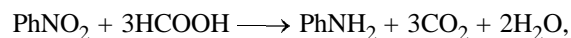
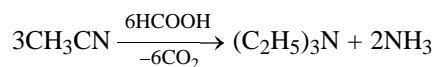
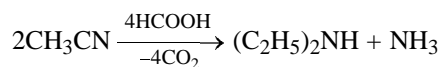
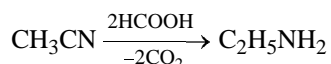
Carbonylation of nitroarenes



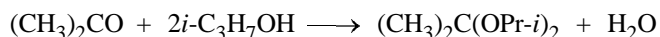
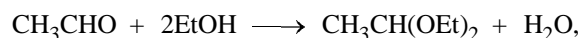
Carbonylation of nitroarenes, coupled with oxidation



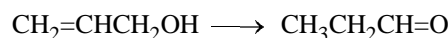
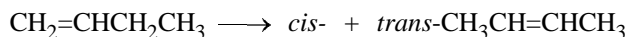
Hydrogenation

(a) under the action of H_2 (b) under the action of HCOOH 

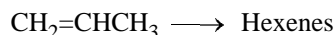
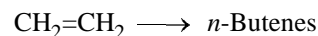
Acetalization of carbonyl compounds



Isomerization of olefins



Oligomerization of olefins



the catalytic solution of such bulky ligands as PPh_3 and phen which are able to strongly coordinate to palladium atoms, have almost no rate effect on olefin oxidation.

At the same time, small extra ligands, such as $\text{C}_2\text{H}_5\text{SH}$, I^- , and SCN^- , effectively inhibit oxidative acetoxylation of ethylene and propylene. As seen from Fig. 4, the oxidation of ethylene is completely blocked when about 50 atoms of an extra ligand have been added to the solution, whereas to completely stop the oxidation of propylene about 15 molecules of inhibitor ligand will suffice [10, 21]. The kinetic data allowed a reaction mechanism to be proposed, where the metal core of a giant cluster plays role of "electronic mediator" [10].

Giant Pd clusters were found to catalyze alkene oxidation with acids, which is unusual with palladium catalysts. The activity of catalysts on the basis of Pd^{II} complexes steeply decreases with increasing solution acidity [22, 23] and is suppressed in the presence of bulky donor ligands like PPh_3 and phen. By contrast, the oxidation of alkenes in aqueous solutions of giant clusters **4** and **5** is practically insensitive to the presence of excess PPh_3 and phen ligands and takes place only in the presence of strong acids (HClO_4 , H_2SO_4 , etc.). Herewith, ethylene is sequentially oxidized to acetaldehyde and acetic acid, and propylene, to allyl alcohol, acrolein, and acrylic acid [24].

Oxidation of alcohols and aldehydes. In the pre-

Table 2. Constants of kinetic equation (3)

Olefin	Cluster	k , min^{-1}	$K_I \times 10^3$, M	$K_{II} \times 10^4$, M	K_{III} , M
Ethylene	4	8.2 ± 0.7	5.8 ± 0.3	3.0 ± 0.2	1.3 ± 0.1
Propylene	5	3.3 ± 0.3	≥ 30	5.2 ± 0.3	0.67 ± 0.05
"	5	5.6 ± 0.5	≥ 30	1.2 ± 0.1	4.8 ± 0.5

Table 3. Kinetic effects at 333 K

Olefin	Catalyst	$k_{C_nH_{2n}} /$ $k_{C_nD_{2n}}$	$k_{CH_3COOH} /$ k_{CH_3COOD}
Ethylene	5	1.1 ± 0.1	1.1 ± 0.1
Propylene	4	2.2 ± 0.2	1.0 ± 0.05
"	5	3.6 ± 0.2	1.0 ± 0.05
"	Pd black	1.0 ± 0.1	2.0 ± 0.2

sence of giant clusters, normal aliphatic alcohols are easily oxidized to aldehydes and esters whose alcohol and acid components contain the same carbon skeleton as in the initial alcohol. Secondary alcohols are oxidized to ketones. With excess alcohol, the resulting carbonyl compounds convert to acetals and ketals, the acetalization reaction being catalyzed with giant palladium clusters [25, 26].

The oxidation of ethanol in anhydrous solvents (MeCN, EtOH, acetone) gives, along with the above products, acetic anhydride as a result of attack of AcOH or AcO^- on the coordinated acyl group $\text{Me}^+\text{C}=\text{O}$ [27].

It was recently found that giant cluster **4** effectively

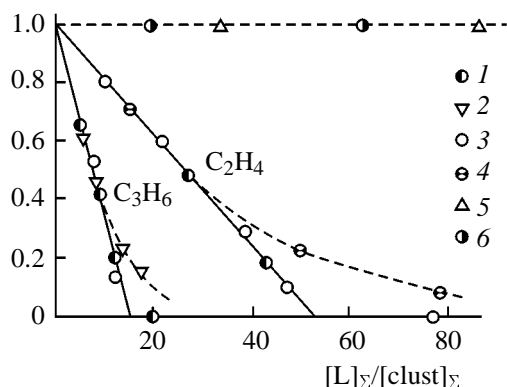
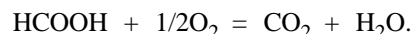


Fig. 4. Effect of inhibiting ligands L on the rate of oxidative acetoxylation of ethylene and propylene in solutions of giant cluster **4**: (1) EtSH; (2) I_2 ; (3) $\text{Et}_2 \cdot \text{NCS}_2\text{Na}$; (4) KSCN; (5) phen; and (6) PPh_3 [21].

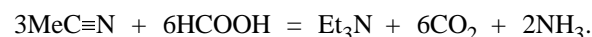
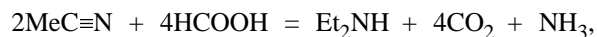
catalyzes the nonradical oxidation of benzyl alcohol with dioxygen to benzaldehyde, but, in contrast with reactions involving aliphatic aldehydes (which further convert to acetals and esters), inhibits further oxidation of benzaldehyde [28].

Oxidation of formic acid. In the presence of oxygen, giant clusters **4** and **5** effectively catalyze oxidation of formic acid:

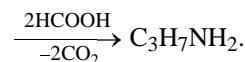


The kinetics of this reaction were studied in detail and its mechanism was suggested [26] (Scheme 4), including, as the limiting stage, coordination of HCOOH molecule, accompanied by C–O bond rupture.

Hydrogenation of multiple bonds with formic acid. Platinoids and their complexes are widely used as catalysts in hydrogenation of multiple bonds ($\text{N}=\text{O}$, $\text{C}=\text{C}$, $\text{C}=\text{O}$) under the action of H_2 and other hydrogen donors: cyclohexene, isopropyl alcohol, and ascorbic and formic acids. In contrast with the majority of substrates, nitriles are scarcely reduced both with molecular H_2 , and with other hydrogen donors. We discovered [27] that nitriles are easily hydrogenated in the presence of giant cluster **4** already at 20°C in the presence of formic acid as hydrogen donor:



The reduction of acrylonitrile with formic acid in methanol solution, catalyzed by cluster **4**, leads to a primary amine in 30% yield. Initially, the $\text{C}=\text{C}$ bond is hydrogenated to form propionitrile which is then hydrogenated to *n*-propylamine:



The hydrogenation of benzonitrile under the action of HCOOH leads to formation of benzylamine and dibenzylamine. Simultaneously, in this system primary amines exceptionally easily convert into secondary and tertiary.



In solutions of giant clusters, nitrobenzene, nitroso-benzene, and phenylhydroxylamine are easily reduced with formic acid to aniline:

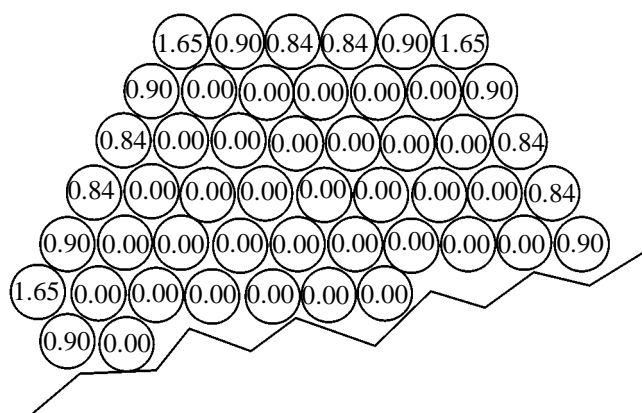


Fig. 5. Positive charge distribution on metal atoms inside the cluster cation $[M_{561}]^{180+}$ (equatorial section) as given by calculations by the electrostatic model [32].

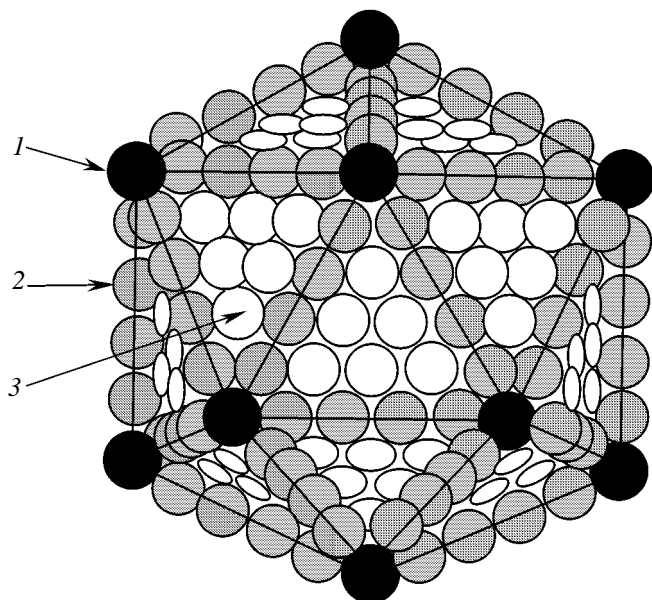
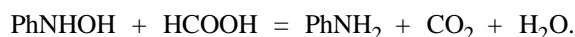
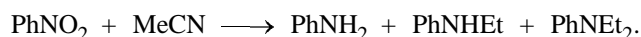


Fig. 6. Distribution of positively charged metal atoms on the surface of the cluster cation $[M_{561}]^{180+}$: (1) the strongest Lewis centers at the vertices of the metal polyhedron; (2) weaker Lewis centers at the edges; and (3) the least electrophilic positively charged metal atoms at the faces [32].

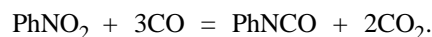
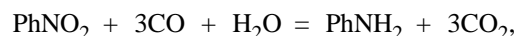


The reduction of nitroarenes in acetonitrile yields much disproportionation products of the corresponding amines:

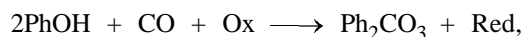


In the same catalytic system, easy hydrogenation $\text{C}=\text{O}$ and $\text{C}=\text{C}$ bonds attached to the benzene ring was observed (Table 1) [29, 30].

Reactions involving CO. Giant palladium clusters effectively catalyze oxidation of CO both with oxygen and with other oxidants, such as nitrobenzene. In the presence of an even small amount of water (2–5 wt %), nitrobenzene is smoothly reduced to aniline. By contrast, the reaction catalyzed by cluster **4** leads to formation of phenyl isocyanate in the absence of H_2O or at its small content (1–2 wt %) [31]:



The same reaction in phenol involves oxidative carbonylation of phenol to diphenyl carbonate simultaneously with reduction of nitrobenzene [31]:



where $\text{Ox} = \text{PhNO}_2$, $\text{Red} = \text{PhNCO}$ or PhNH_2 (3 h, 140 at, 150°C , yield 200 mol per mole cluster). In this reaction, the giant cluster catalyzes coupling of two redox processes: reduction of nitro compound and oxidative carbonylation of phenol.

Reactions of aldehydes. Giant clusters do not belong to strong acids or bases. Nevertheless, it was found that clusters **4** and **5** can catalyze reactions typical of acid–base catalysis, for example, acetalization of carbonyl compounds under the action of alcohols in neutral solutions ($20\text{--}50^\circ\text{C}$) [26].

The occurrence of typical acid-catalyzed reactions suggests that giant palladium clusters not only mediate electron transfer in redox reactions, but also can serve as Lewis acids.

Table 4. Positive charge distribution on the surface layer of “magic-number” metal clusters

n	N_Σ	N_{ext}	N_{ver}	N_{edge}	N_{face}
2	55	42	+0.54	+0.33	+0.24
3	147	92	+0.87	+0.48	+0.24
4	309	162	+1.26	+0.66	+0.33
5	561	252	+1.65	+0.84	+0.42
6	923	362	+2.04	+1.02	+0.48
7	1415	492	+2.49	+1.20	+0.55

^a (n) Number of layers, (N_Σ) total number of atoms, (N_{ext}) number of atoms in the external layer, (N_{ver}) atomic charge in the vertex, (N_{edge}) atomic charge in the middle of the edge, and (N_{face}) atomic charge in the center of the face.

In accordance with the Gauss theorem, the charge on a sufficiently large metallic particle (here cluster metal core) should be distributed over its surface. In the case of a spherical particle, the charge is uniformly distributed over the surface layer of the metal core, whereas metal atoms inside the metal core are neutral. However, the metal core in the idealized giantcluster model corresponding to experimental data [4, 5] has the shape of isosahedron or cubic octahedron. In this case, one can expect that some atoms carry a higher charge (to be more electrophilic), while the rest atoms are charged to a lesser extent (to be less electrophilic).

In this connection, we carried out search for a minimum of the potential energy of electrostatic interaction between charged particles composing the cluster metal core, as a function of charge distribution between the particles, within the frames of a simple electrostatic model. The cationic clusters of Chini's series [15] were considered, with "magic" numbers of metal atoms: M_{55} , M_{147} , M_{309} , M_{561} , M_{923} , and M_{1415} , and constructed of 12-vertex metal polyhedra: cubic octahedron, anticubic octahedron, or icosahedron, formed by densely packed conducting spheres (metal atoms).

In accordance with the chemical composition of clusters **4** and **5**, the average formal positive charge z_i per one metal atom is $z_i = +180:561 \approx +0.31$. Approximately the same value corresponds to the average charge (per one metal atom) of "magic-number" cluster cations $[M_{55}]^{17+}$, $[M_{147}]^{47+}$, $[M_{309}]^{99+}$, $[M_{561}]^{180+}$, $[M_{923}]^{296+}$, and $[M_{1415}]^{454+}$. The goal of calculations consisted in finding the electrical charge distribution corresponding to a minimum of the total electrostatic energy of the cluster system.

Numerical solution by successive (iterative) redistribution of electric charge, in small portions, between nearest neighbors [32] showed that the potential energy minimum corresponds to a charge distribution where metal atoms in all inner layers of the cluster are electroneutral, whereas the whole positive charge is distributed over the surface layer of the metal core (Fig. 5).

The metal atoms at the vertices of the metal polyhedron carry the highest positive charge (Table 5, Fig. 6).

As the cluster size increases, the charge of vertex metal atoms steeply grows attaining about +2 already in the case of a 923-atomic cluster with 6 layers. Even for a typical 5-layer cluster M_{561} , this charge essentially exceeds the cluster average value of +0.3, practically approaching the formal charge of divalent

metal ions in acido complexes like $PdCl_4^{2-}$ or $Pd_3(OAc)_6$. Therefore, one can suppose that vertex atoms of cluster polyhedra are electrophilic enough to effect catalytic activation of alcohols, aldehydes, and alkenes. By contrast, the positive charge of the metal atoms at the edges and, especially, at the faces of the metal polyhedron is considerably lower (Fig. 2).

For steric reasons and in accordance with the geometry of the idealized structure of clusters **4** and **5**, phen ligands are bound with the Pd atoms located at the vertices and partly at the edges of the metal polyhedron [5, 11]. Our estimates (Table 1) show that it is these Pd atoms that are the most electrophilic. Analysis of the idealized structure shows that the cluster surface is almost completely shielded by phen ligands, except for 2–3 Pd atoms at the faces of the metal polyhedron. According to our data, those metal atoms which are most sterically accessible for oxidative activation of substrates (CO, ethylene, propylene, etc.) are the least electrophilic. One can believe this circumstance is of no special importance for redox reactions whose first act probably involves coordination or oxidative addition of substrate by the Pd–Pd bond. The rupture of the metal–metal bond, produced by coordination of alkene or CO, proceeds the easier, the lower the positive charge on the metal atoms: The bond energy in the cation $[Pd-Pd]^+$ is 39 ± 12 kcal/mol, and in the neutral molecule Pd–Pd it is as low as 15 ± 5 kcal/mol[33].

The above results provide an only qualitative estimate of the charge distribution in the metal core of large metal clusters. Our simplified model relates to nonligand metal clusters with the idealized geometry in the form of a regular 12-vertex metal polyhedron. Real molecules of giant clusters (for example, of the Pd_{561} family: clusters **4**, **5**, and their analogs) deviate from the idealized form in a greater or lesser degree.

According to HREM data [13, 34], only a small fraction of real molecules of clusters **4** and **5** have a metal core in the form of regular cubic octahedron or of multiple twins with a 5-fold axis close to regular icosahedron. A considerable fraction of clusters more or less deviate in shape from ideal; there are both truncated vertices and sharp peaks on their surfaces. Naturally, the positive charges of such "defective" sites appreciably differs from those for a regular 12-vertex polyhedron.

Nevertheless, even at a qualitative level, the resulting data suggest the possibility of existence of Lewis acid centers on the surface of giant metal clusters. The acid catalysis by giant clusters like **4** and **5** seems to be effected by the Pd atoms located at surface defects, such as vertices devoid of phen ligands, adsorbed metal atoms, vicinities of truncated vertices, etc.

CONCLUSION

Giant palladium clusters make an example of objects for which a strategy was first formulated, based on the use of indirect methods for structural assessment of the poorly explored colloidal metals. Studying giant clusters in terms of this approach would not only allow quantum-size effects in the properties of these nanoparticles to be revealed, but also catalysts and catalytic systems to be suggested to open new selective ways for performing industrially important reactions.

ACKNOWLEDGMENTS

The work was financially supported by the Russian Foundation for Basic Research (project no. 99-03-32292).

REFERENCES

- Faraday, M., *Phil. Trans. Roy. Soc.*, 1857, vol. 147, pp. 145–153.
- Graham, T., *Phil. Trans. Roy. Soc.*, 1861, vol. 151, pp. 183–190.
- Ponec, V. and Bond, G.C., *Studies in Surface Sciences and Catalysis*, Delmon, B. and Yates, J.T., Eds., *Catalysis by Metals and Alloys*, Amsterdam: Elsevier, 1995, vol. 95, p. 734.
- Vargaftik, M.N., Zagorodnikov, V.P., Stolyarov, I.P., Likholobov, V.A., Chuvilin, A.L., Zaikovskii, V.I., Kochubei, D.I., Timofeeva, G.I., Zamaraev, K.I., and Moiseev, I.I., *Dokl. Akad. Nauk SSSR*, 1985, vol. 284, pp. 896–899.
- Vargaftik, M.N., Zagorodnikov, V.P., Stolyarov, I.P., Moiseev, I.I., Kochubei, D.I., Chuvilin, A.L., Zaikovskii, V.I., Zamaraev, K.I., and Timofeeva, G.I., *J. Chem. Soc. Chem. Commun.*, 1985, pp. 937–938.
- Stromnova, T.A., Kuz'mina, L.G., Vargaftik, M.N., Mazo, G.Ya., Struchkov, Yu.T., and Moiseev, I.I., *Izv. Akad. Nauk SSSR, Ser. Khim.*, 1978, pp. 720–723.
- Vargaftik, M.N., Stromnova, T.A., Khodashova, T.S., Porai-Koshits, M.A., and Moiseev, I.I., *Koord. Khim.*, 1981, vol. 7, pp. 132–134.
- Moiseev, I.I., *Palladium Clusters in Catalysis, Chemistry Reviews (Sov. Sci. Rev., Sect. B)*, Volpin, M.E., Ed., New York: Harwood Acad., 1982, pp. 1–35.
- Vargaftik, M.N., Zagorodnikov, V.P., Stolyarov, I.P., Kochubei, D.I., Nekipelov, V.M., Mastikhin, V.M., Chinakov, V.D., Zamaraev, K.I., and Moiseev, I.I., *Izv. Akad. Nauk SSSR, Ser. Khim.*, 1985, pp. 2381–2389.
- Vargaftik, M.N., Zagorodnikov, V.P., Stolyarov, I.P., Moiseev, I.I., Kochubei, D.I., Likholobov, V.A., Chuvilin, A.L., and Zamaraev, K.I., *J. Mol. Catal.*, 1989, vol. 53, pp. 315–353.
- Vargaftik, M.N., Moiseev, I.I., Kochubei, D.I., and Zamaraev, K.I., *Faraday Discuss.*, 1991, vol. 92, pp. 13–42.
- Volkov, V.V., Van Tendeloo, G., Vargaftik, M.N., Stolyarov, I.P., and Moiseev, I.I., *Mendeleev Commun.*, 1993, pp. 187–189.
- Volkov, V.V., van Tendeloo, G., Tsirkov, G.A., Cherkashina, N.V., Vargaftik, M.N., Moiseev, I.I., Novotortsev, V. M., Kvit, A.V., and Chuvilin, A.L., *J. Cryst. Growth*, 1996, vol. 163, p. 377.
- Moiseev, I.I., Vargaftik, M.N., Volkov, V.V., Tsirkov, G.A., Cherkashina, N.V., Novotortsev, V.M., Ellert, O.G., Petrunenko, I.A., Chuvilin, A.L., and Kvit, A.V., *Mendeleev Commun.*, 1995, pp. 87–89.
- Chini, P., *J. Organomet. Chem.*, 1980, vol. 200, pp. 37–54.
- Mackay, A.L., *Acta Crystallogr.*, 1961, vol. 15, pp. 916–920.
- Teo, B.K. and Sloan, N.J.A., *Inorg. Chem.*, 1985, vol. 24, pp. 4545–4557.
- Zagorodnikov, V.P., Vargaftik, M.N., Kochubei, D.I., Likholobov, V.A., Kolomiichuk, V.N., Naumochkin, A.N., Chuvilin, A.L., Novotortsev, V.M., Ellert, O.G., and Moiseev, I.I., *Izv. Akad. Nauk SSSR, Ser. Khim.*, 1989, pp. 849–854.
- Poulin, C., Kagan, H.B., Vargaftik, M.N., Stolyarov, I.P., and Moiseev, I.I., *J. Mol. Catal. A*, 1995, vol. 95, pp. 109–114.
- Volokitin, Ya., Sinzig, J., de Jongh, L.J., Schmid, G., Vargaftik, M.N., and Moiseev, I.I., *Nature*, 1996, vol. 384, pp. 621–622.
- Stolyarov, I.P., Vargaftik, M.N., and Moiseev, I.I., *Kinet. Katal.*, 1987, vol. 28, pp. 1359–1363.
- Moiseev, I.I., *π -Komplekсы в жидкофазном окислении олефинов* (π Complexes in Liquid-Phase Oxidation of Olefins), Moscow: Nauka, 1970, p. 273.
- Moiseev, I.I., Levanda, O.G., and Vargaftik, M.N., *J. Am. Chem. Soc.*, 1966, vol. 88, pp. 3491–3495.
- Pasichnyk, P.I., Starchevsky, M.K., Pazdersky, Yu.A., Zagorodnikov, V.P., Vargaftik, M.N., and Moiseev, I.I., *Mendeleev Commun.*, 1994, no. 1, pp. 1–3.
- Starchevskii, M.K., Gladkii, S.L., Lastoviyak, Ya.V., Pasichnyk, P.I., Pazderskii, Yu.A., Vargaftik, M.N., and Moiseev, I.I., *Kinet. Katal.*, 1996, vol. 37, no. 3, pp. 408–415.

26. Moiseev, I.I. and Vargaftik, M.N., *Perspectives in Catalysis*, Thomas, J.A. and Zamaraev, K.I., Eds., Oxford: Blackwell, 1992, pp. 91–123.
27. Moiseev, I.I., Tsirkov, G.A., Gekhman, A.E., and Vargaftik, M.N., *Mendeleev Commun.*, 1997, no. 1, pp. 1–3.
28. Gladkii, S.L., Starchevskii, M.K., Pazderskii, Yu.A., Vargaftik, M.N., and Moiseev, I.I., *Izv. Akad. Nauk SSSR, Ser. Khim.*, 2001, no. 5, pp. 881–882.
29. Moiseev, I.I. and Vargaftik, M.N., *Catalysis by Di- and Polynuclear Metal Cluster Complexes*, Adams, R.D. and Cotton, F.A., Eds., New York: Wiley-VCH, 1998, pp. 395–442.
30. Vargaftik, M.N., Kozitsyna, N.Yu., Cherkashina, N.V., Rudyi, R.I., Kochubei, D.I., Novgorodov, B.N., and Moiseev, I.I., *Kinet. Katal.*, 1998, vol. 39, no. 6, pp. 806–824.
31. Moiseev, I.I., Vargaftik, M.N., Chernysheva, T.V., Stromnova, T.A., Gekhman, A.E., Tsirkov, G.A., and Makhlina, A.M., *J. Mol. Catal. A*, 1996, vol. 108, pp. 77–85.
32. Abramova, L.A., Baranov, S.P., Dulov, A.A., Vargaftik, M.N., and Moiseev, I.I., *Dokl. Akad. Nauk*, 2001, vol. 377, pp. 344–347.
33. *Energii razryva khimicheskikh svyazei. Potentsyaly ionizatsii i srodstvo k elektronu* (Dissociation Energies of Chemical Bonds. Ionization Potentials and Electron Affinity), Kondrat'ev, V.N., Ed., Moscow: Nauka, 1974, p. 39.
34. Oleshko, V., Volkov, V., Gijbels, R., Jacob, W., Vargaftik, M., Moiseev, I., and Van Tendeloo, G., *Z. Phys. D*, 1995, vol. 34, pp. 283–289.